*Particle Accelerators*, 1997, Vol. 58, pp. 241–255
Reprints available directly from the publisher
Photocopying permitted by license only



# MICROWAVE INSTABILITY AND IMPEDANCE MEASUREMENTS IN THE CERN SPS

T. LINNECAR and E. SHAPOSHNIKOVA*

*CERN, Division SL, 1211 Geneva 23, Switzerland*

*(Received in final form 4 March 1997)*

The single bunch intensity of protons in the SPS is limited by the microwave instability. The main sources of the SPS impedance responsible for this instability have been determined by measurements of the spectrum of unstable single bunches injected into the machine. New experimental data and the improved impedance model have helped to explain some previously contradictory results concerning the microwave instability threshold – one of the critical parameters for the SPS as LHC injector. Ways of curing the instability are discussed.

*Keywords:* Microwave instability; Impedance

## 1 INTRODUCTION

The purpose of this work is to analyse both previously published and more recently obtained experimental data on the longitudinal microwave instability in the SPS. This instability was observed in the SPS already in 1977[1] with protons and then later with leptons as well. The threshold was raised by using a lower frequency RF system (100 MHz instead of 200 MHz) to capture longer bunches. For present fixed target proton operation in the SPS this instability is not harmful due to relatively low ($10^{10}$) bunch density. However, the threshold of this instability, when estimated by scaling from previous measurements[2] was found to be the most critical factor in the choice of parameters for the SPS when used as LHC injector.[3]

* Corresponding author. E-mail: Elena.Chapochnikova@cern.ch.

The nominal intensity of a single bunch for the LHC beam is $10^{11}$, (the ultimate intensity is 1.7 times higher). The threshold for the microwave instability found[2] for a bunch with length $\tau = 3.5$ ns and longitudinal emittance $\varepsilon = 0.47$ eV s is $\sim 9 \times 10^{10}$. The bunch which will be injected into the SPS after the modifications foreseen to the PS RF, should have[4] $\tau = 4$ ns and $\varepsilon = 0.35$ eV s. The bunch lengths in these two cases are very similar; however, the momentum spread of the LHC beam is 30% smaller. If one scales from these measurements to the LHC beam parameters according to the Keil–Schnell–Boussard criterion[5] a threshold approximately twice less than the nominal intensity is found.

Another set of experimental data previously obtained,[6] also for a similar bunch length (5 ns) but at a different energy and with RF off, gives the threshold for the microwave instability, after scaling, close to the ultimate LHC bunch intensity.

To clarify the situation and prepare the SPS as injector for the LHC, a new series of measurements was started 2 years ago. Before the end of 1998 it will not be possible to eject bunches from the PS into the SPS with all the parameters as proposed for the LHC; nevertheless, the bunch lengths can be very close (4.5–5 ns). These measurements need special cycles in the SPS and its injectors. The analysis of the results of measurements made using dedicated machine development sessions in 1995[7] and a parasitic cycle interleaved with the physics cycles in 1996[8] is presented below.

## 2 MEASUREMENTS OF THE INSTABILITY THRESHOLD

The longitudinal microwave instability is observed in the SPS as intensity-dependent bunch lengthening associated with strong beam signals at high frequencies. Traditional methods to measure the microwave instability threshold are based on these phenomena. In our experiments we also used both approaches – measurements of bunch length and spectrum.

Since the bunches ejected from the PS are at the moment too long for clean capture into a 200 MHz bucket (the RF system to be used with the LHC beam), a 100 MHz system was used to measure the instability threshold with RF on. We made measurements at two

different RF voltages – one calculated to be matched for the low intensity bunch (150 kV) and the second twice more. The results are presented in Figures 1–3.

In Figure 1 we show the bunch length at 1.5 s after injection as a function of intensity measured both at the bottom of the current distribution ($\tau$) and at its half height ($\tau_{\text{fwhh}}$). The lowest intensity points on these graphs were estimated as the average of the initial bunch lengths at injection, i.e. before being affected by the SPS machine. As can be seen the initial bunch length has almost 10% scatter. We also observed the dependence of the bunch length at injection from the

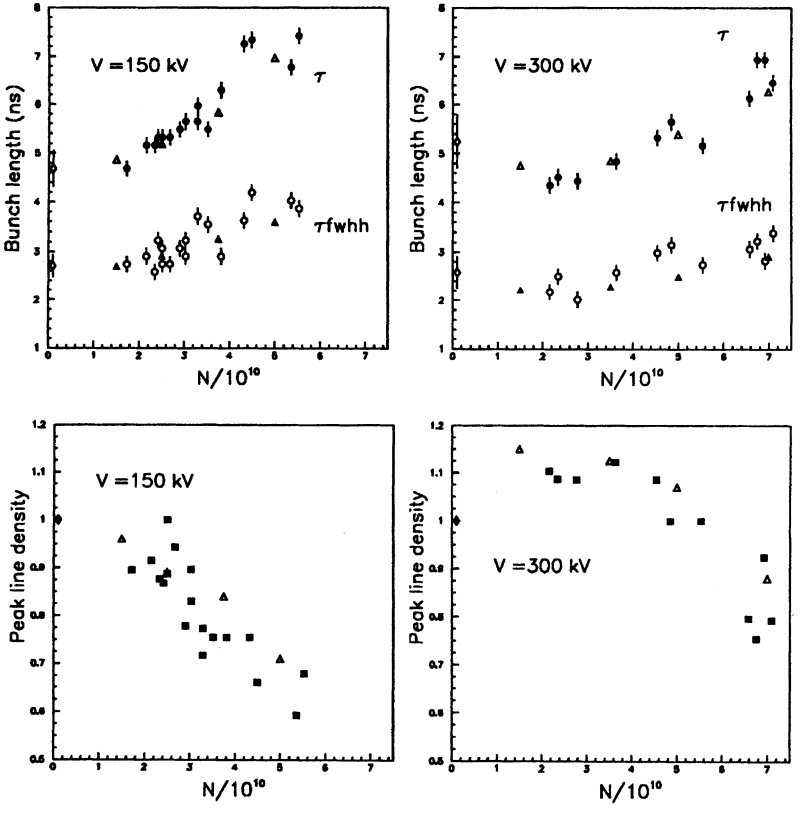


FIGURE 1 Bunch length (circles, top) and peak line density normalised to its initial value (squares, bottom) measured as a function of intensity after 1.5 s for bunches captured in 100 MHz RF system with $V = 150$ kV and $V = 300$ kV. Triangles show results of numerical simulations discussed in Section 3.

PS on the intensity (this changed on average by 5% over the range of intensities available). Unlike the previous measurements[2] where the beam intensity was changed by scraping after ejection from the PS, the intensity in our experiment was varied in the injectors.

In Figure 1 we also present the ratio of the bunch peak line density measured after 1.5 s to that at injection as a function of intensity. The peak is measured from bunch profiles obtained from a wide band longitudinal pickup. The measurements with the lower voltage suggest a threshold of $(2-3) \times 10^{10}$, at which point the character of the dependence on intensity is obviously changing.

The other common method that is used to define the microwave instability threshold is based on the observation of beam signals at high frequencies. In our first experiments we measured the detected microwave signal from the wide band monitor using a bandpass filter in the range 1.3–1.6 GHz. In Figure 2 we give the maximum amplitude of this microwave signal measured during the first 50 ms after injection when captured in the 100 MHz RF system with $V = 150$ kV and also 300 kV. Signals were observed in both cases even at the lowest intensities.

In Figure 3 we present the instability start time measured as the onset of microwave signals for the same bunches but this time injected into the machine with RF off. In this case for intensities of

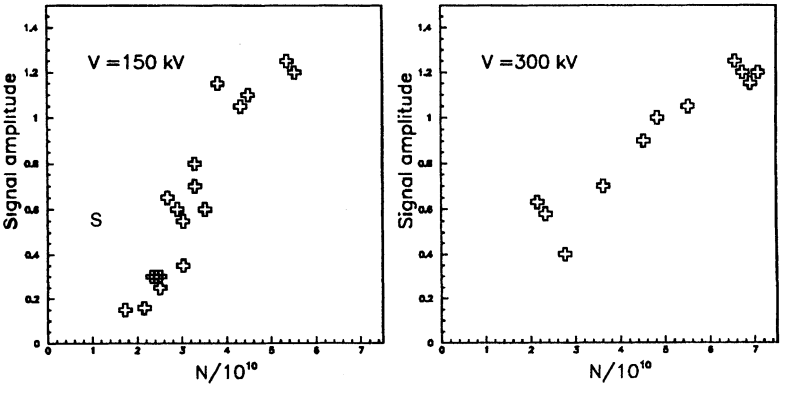


FIGURE 2 Amplitude of the high frequency signal (1.3–1.6 GHz) measured as a function of intensity for bunches captured in the 100 MHz RF system with $V = 150$ kV and $V = 300$ kV.

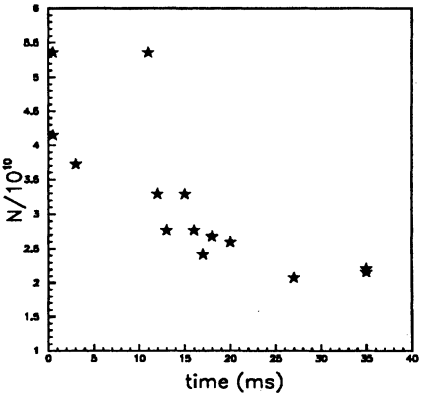


FIGURE 3 Intensity versus instability start time during debunching.

$5 \times 10^{10}$ the microwave signal appeared 2–3 ms after injection. As the intensity was lowered to $1 \times 10^{10}$, the signal grew after a progressively longer period of time, up to 50 ms.

Some conclusions that one can derive from the data presented in Figures 1–3 are:

- From bunch lengthening and peak line density measurements (Figure 1) the threshold intensity $N_{\text{th}}$ is $\sim 2.5 \times 10^{10}$ for capture with 150 kV voltage and definitely higher, $\geq 4 \times 10^{10}$, for 300 kV voltage.
- For the case with RF on, the threshold intensity determined from the measurements of the amplitude of the microwave signal, to within the available accuracy, is similar for the two voltages ($\sim 2$–$3 \times 10^{10}$); however, from measurements with RF off this threshold is approximately twice as high. From this point of view our results have confirmed the discrepancy in the other data.[2,6]

To compare the results of the various threshold measurements let us first apply the broad band resonator model of the SPS that has been widely used in the past. For the case when the width of the bunch spectrum ($\sim 1/\tau$) is much narrower than the width of the impedance, the criterion for the fast microwave instability can be written in the form[5]

$$\frac{|Z|/n}{F^*} \leq \frac{pc\beta|\eta|}{e^2 N_{\text{th}}} \left(\frac{\Delta p}{p}\right)^2 \tau, \tag{1}$$

where $Z/n$ is the longitudinal impedance, $\pm\Delta p$ is the maximum momentum spread, $\tau$ is the bunch length, $N_{\text{th}}$ is the number of particles per bunch at the threshold of instability, $F^*$ is a formfactor taking into account different particle distributions, $\eta = 1/\gamma_t^2 - 1/\gamma^2$, $\gamma$ and $\gamma_t$ are the relativistic factor at synchronous and transition energy respectively, $p$ is the synchronous momentum and $\beta$ is the velocity in units of the velocity of light.

The bunch parameters together with the value of $|Z|/(nF^*)$ calculated from (1), of both the previous and recent threshold measurements for protons and for leptons,[9] are summarised in Table I.

For the leptons the threshold measurements were based on the observation of the high frequency signal. This instability was recorded only at injection. The threshold during the cycle estimated from (1) suggested a strong intensity limitation at higher energies which was never confirmed.

Even taking into account differences in particle distribution, there is no surprise in finding that the estimations of the SPS broad band impedance based on the different measurements in Table I give a value for $|Z|/n$ in the range 10–40 Ω.

In the framework of the broad band impedance model the best fit (not shown) to the measurements presented in Figure 1, was obtained using a resonator with $R_{\text{sh}} = 300\,\text{k}\Omega$ and the typical values of $Q = 1$ and $f_r = 1.35\,\text{GHz}$ assumed previously, which is equivalent to $|Z|/n = 10\,\Omega$. To fit the curve we used results obtained by numerical simulation with the code ESME.[10] However, this model is not able to explain simultaneously the data for the intensity dependence of both $\tau$ and $\tau_{\text{fwhh}}$ given in Figure 1, nor the data given in Figure 3. It is clear that the broad band impedance model is too simplified. An

TABLE I Measurements of microwave instability threshold in the SPS

| Ref. number | $f_{\text{rf}}$ (MHz) | $p$ (GeV/$c$) | $\gamma_t$ | $\tau$ (ns) | $\varepsilon$ (eV s) | $(\Delta p/p)/10^{-3}$ | $N_{\text{th}}/10^{10}$ | $\lvert Z\rvert/nF^*$ (Ω) |
|---|---|---|---|---|---|---|---|---|
| 2 | 200 | 26.0 | 23.4 | 3.5 | 0.47 | 3.2 | 8.5 | 37.1 |
| 6 | off | 15.8 | 14.4 | 5.0 | 0.15 | 1.2 | 10.0 | 9.1 |
| 7 | 100 | 26.0 | 23.4 | 5.0 | 0.2 | 1.0 | 2.5 | 18.6 |
| 7 | off | 26.0 | 23.4 | 5.0 | 0.2 | 1.0 | 5.0 | 9.4 |
| 9 | 100 | 3.5 | 23.4 | 4.0 | 0.04 | 2.0 | 3.5 | 18.0 |
| LHC | 200 | 26.0 | 23.4 | 4.0 | 0.35 | 2.0 | | |

attempt to produce an impedance model based on the analysis of the hardware in the SPS had been made in Ref. 11, where contributions to the low frequency machine impedance coming from different machine elements were estimated, and which gave $Z/n = 7\,\Omega$. Below we present the results from recent measurements which have allowed the main components of the SPS impedance to be observed with the beam in the frequency range from 100 MHz to 4 GHz.

## 3 MEASUREMENTS OF THE IMPEDANCE WITH THE BEAM

In our latest measurements concerning the microwave instability in the SPS we used a new technique which is described in more detail in Ref. 8. Below we present a brief description of the method and the main results obtained.

This method is based on the measurement of the spectrum of unstable bunch modes. In our experiments single high intensity proton bunches were injected into the machine with RF off and their spectrum observed during slow debunching. The presence of different resonant impedances leads to line density modulation at the resonant frequencies. This instability reaches some maximum modulation amplitude which was recorded as a function of frequency for many different bunches. We scanned the frequency from 100 MHz to 4 GHz using a spectrum analyser with a bandwidth of 3 MHz as a receiver. The signal was taken from the wall current pickup.[12] At each frequency point the maximum amplitude of the detected signal within the first 100 ms after injection was recorded. The data was taken for at least ten different bunches and then averaged.

The results of these measurements done at 26 GeV/$c$ with bunches having length $\tau = 25$ ns and emittance $\varepsilon = 0.25$ eV s are shown in Figure 4(a), where numerous peaks corresponding to different impedances in the machine can be seen. With this choice of bunch parameters the debunching time, defined as

$$t_d = \frac{\tau(0)}{2|\eta|[\Delta p(0)/p]}, \tag{2}$$

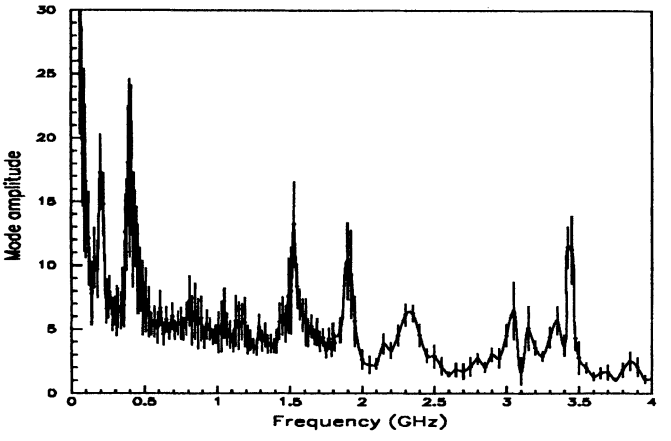


(a)

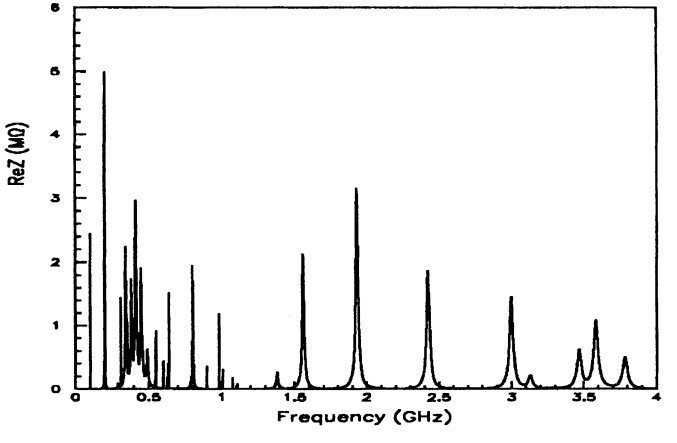


(b)

FIGURE 4 Measured spectrum of unstable bunches, top, and resistive part of longitudinal impedance of different elements in the SPS, bottom.

is 80 ms. This means that the increase in bunch length, approximately described by the formula

$$\tau(t) = \tau(0)\sqrt{1 + t^2/t_d^2}, \tag{3}$$

did not exceed 60% during the first 100 ms.

To analyse the instability threshold in the previous section we used the broad band impedance[5] criterion which is applicable[15] only if the resonant impedance bandwidth is much wider than the width of bunch spectrum. From the measurements presented in Figure 4(a) and analysis of the hardware it appears that for most of the dominant impedances in the SPS the opposite is true, so that $1/\tau \gg f_r/(2Q)$. Below we will call this case "narrow band impedance".

For a fast instability with a growth time smaller than the synchrotron period in the case with RF on, or the debunching time in the case with RF off, the spectrum of an unstable bunch mode $\rho_n$ associated with the narrow band impedance centred at frequency $f_r = n_r f_0 = \omega_r/(2\pi)$ can be found from linear theory:[8]

$$\rho_n \sim nG(n - n_r), \tag{4}$$

where

$$G(n) = \int_{-\pi}^{\pi} \lambda(\theta) e^{in\theta} d\theta \tag{5}$$

is the Fourier transform of the initial line density distribution $\lambda(\theta)$. Here $f_0$ is the revolution frequency and $\theta$ is the azimuthal coordinate along the circumference.

As can be seen from (4) the mode spectrum has a centre frequency close to the resonant frequency of the impedance. The spectrum width, to a first approximation, is defined only by the bunch distribution and is proportional to $1/\tau$. Thus with sufficiently long bunches the fine structure of the machine impedance can be resolved in frequency.

The growth rate of the instability in this approximation is

$$\operatorname{Im} \Omega \simeq \omega_r \left( \frac{Ne^2 \omega_0 |\eta|}{16\pi E_0} \frac{R_{sh}}{Q} \right)^{1/2}. \tag{6}$$

Since the instability growth rate is proportional to $(R_{sh}/Q)^{1/2}$, the method of measurement described above allows the impedances with high $R_{sh}/Q$ in the machine to be seen with the beam. The confirmation for this approach was also obtained by numerical simulation.

The next step was to identify the different impedances seen with the beam in Figure 4(a) with sources in the machine elements. In Figure 4(b) we show the real part of each resonant longitudinal mode found in the SPS by hardware measurements or calculations (for more details see Ref. 13). Some of them were known before. To this category belong the peaks at 200 and 800 MHz corresponding to the fundamental frequencies of the two travelling wave RF systems in the SPS which have low $Q$ but high $R_{sh}/Q$ values. The peak at 400 MHz was identified later as the impedance introduced by the 16 extraction septa. All the peaks above 1.4 GHz can be explained by the impedance of the 800 vacuum ports which are cavity-like objects. The real part of this latter impedance as given in Figure 4(b) was calculated with MAFIA.[14] The $TM_0$ modes of such an object have a maximum $R_{sh}/Q = 45\,\Omega$ at 1.9 GHz which for 800 units gives 36 kΩ total impedance. All these accidental cavities have two ceramic resistors which lower the value of $Q$ on average by a factor 10. This damped impedance does not lead to coupled bunch instabilities but is a source for the single bunch instability where the unchanged value of $R_{sh}/Q$ is important. The contribution of vacuum ports to the low frequency impedance is relatively small ($Z/n \sim 2.4\,\Omega$).

The measured spectrum in Figure 4(a) determines the frequency of the different resonant impedances in the machine but the amplitude of the peak is not directly proportional to $R_{sh}/Q$. We used numerical simulations to model the measurements of maximum amplitude of the signal reached during the instability, and analytical estimations for its linear part (thresholds and growth rates).

Due to the complicated structure of the signal in time the growth rate of the instability is in general ill-defined in comparison to the maximum amplitude. Nevertheless, we made an attempt to estimate impedances at known frequencies from growth rate measurements in specially selected cases which had a well-defined linear part of instability growth. For five shots with $N = 2 \times 10^{10}$ the average e-folding time is about 6 ms both at $f = 200$ MHz and $f = 400$ MHz. Using formula (6) gives $R_{sh}/Q = 50$ kΩ at 200 MHz and $R_{sh}/Q = 12$ kΩ at 400 MHz. However, these results have a huge scatter due to the quadratic dependence of $R_{sh}/Q$ on growth rate.

Analytical solutions for instability thresholds can be found,[15,16] for a fast instability on a bunch with Gaussian distribution in the limiting

cases of a broad band or narrow band impedance. These can be presented in one generalised form as[†]

$$R_{\mathrm{sh}} \frac{\overline{\Delta f}}{f_{\mathrm{r}}} < \frac{|\eta| pc\beta}{I_{\mathrm{b}}} \left(\frac{\Delta p}{p}\right)^2, \tag{7}$$

where $\overline{\Delta f}$ is defined by the overlapping frequency band of the bunch and impedance spectra and for a Gaussian beam is given by

$$\overline{\Delta f} = \begin{cases} f_{\mathrm{r}}/Q & \text{if } \tau f_{\mathrm{r}} \ll Q, \text{ narrow band impedance,} \\ 1/\tau & \text{if } \tau f_{\mathrm{r}} \gg Q, \text{ broad band impedance.} \end{cases} \tag{8}$$

In the above, $I_{\mathrm{b}}$ is the average beam current, $\tau \simeq 4\sigma_t$ and $\Delta p \simeq 2\sigma_p$, where $\sigma_t$ and $\sigma_p$ are the standard deviation in the time and momentum coordinates. As well as for the growth rate (see (6)), for the threshold of a single bunch instability defined by the interaction with a narrow band resonator it is the value of $R_{\mathrm{sh}}/Q$ and average beam current which is important, and not $R_{\mathrm{sh}}/n_{\mathrm{r}}$ and peak current which are relevant for a broad band impedance. The transition between the two regimes occurs when $f_{\mathrm{r}}\tau \sim Q$.

As far as the instability corresponds to the narrow impedance case, damping the resonators does not help much since $R_{\mathrm{sh}}/Q$ stays constant. The situation becomes different if the broad band impedance regime is reached. Then decreasing $Q$ (and $R_{\mathrm{sh}}$) raises the threshold.

We have attempted also to measure directly the thresholds given by the dominant narrow band impedances in Figure 4(a). In Figure 5 we present the measurements of maximum signal amplitude, as defined before, as a function of intensity which were made at the frequencies of these impedances. Now, if we assume that the instabilities developing at different frequencies do not affect each other, we can try to estimate the impedance from the instability threshold observed at each different frequency. Applying the narrow band impedance criterion (7) we get the following:

[†] Note that the results for the microwave instability thresholds obtained in Ref. 17, from mode coupling theory, with a different particle distribution can also be rewritten in a form similar to Eq. (7).

| Frequency (MHz) | $N_{th}/10^{10}$ | $R_{sh}/Q$ kΩ from $N_{th}$ and (7) | $R_{sh}/Q$ kΩ from hardware |
|---|---|---|---|
| 200 | $\leq 0.6$ | $\geq 21$ | 26.4 |
| 400 | $\approx 1.5$ | 8.5 | — |
| 800 | $\approx 2.5$ | 5.1 | 6.5 |
| 1560 | $\approx 1.1$ | 12 | 21.7 |

Note that for the highest frequency, the width of the spectrum for the 25 ns long bunches used for these measurements becomes comparable with the resonator bandwidth.

For comparison, in Figure 6 we show results obtained at 200 and 800 MHz by numerical simulation using $R_{sh}/Q$ values calculated from the hardware and average initial bunch parameters from the measurements shown in Figure 5. The data from the simulations were treated in a similar way to the experimental data.

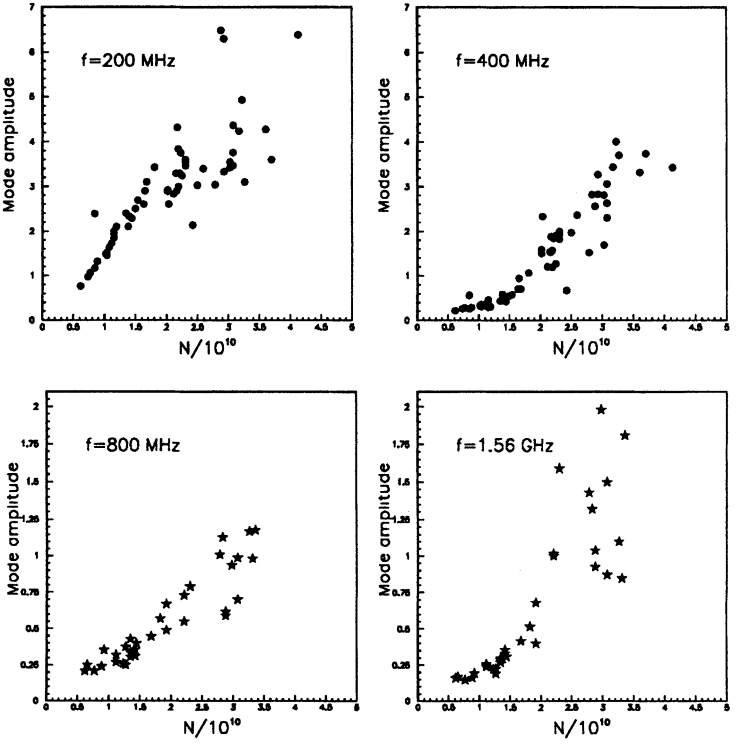


FIGURE 5 Measured amplitude of the signal as a function of intensity at different frequencies for bunches with $\tau = 25$ ns and $\varepsilon = 0.25$ eV s.

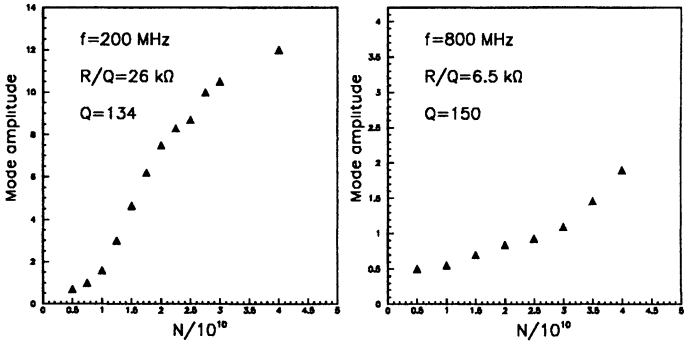


FIGURE 6 Amplitude of the signal (in arbitrary absolute units) as a function of intensity at different frequencies for bunches with $\tau = 25$ ns and $\varepsilon = 0.25$ eV s obtained from numerical simulations.

The impedance model of the SPS containing all the main contributions found from the beam measurements is still developing. It needs some refinement, especially for the low frequency components (400 MHz), which we are doing by measurements in the laboratory.

Bunch lengthening experiments contain the integrated information about the total impedance and we are using them to check our impedance model by numerical simulation. The model containing the impedances from the four main elements (travelling wave RF systems at 200 and 800 MHz, extraction septa and vacuum ports) and consisting of 12 resonant peaks have been used in simulations to reproduce the bunch lengthening measurements in Figure 1. For most elements we used the $R_{sh}/Q$ values found from calculations, and for the $Q$ we used values from laboratory measurements (they are summarised in Ref. 13). For the extraction septa we used $R_{sh}/Q$ estimated from measurements with the beam. Bunch parameters in simulation are the average initial bunch parameters from the measurements in Figure 1. The results of simulations are shown in Figure 1 as triangles. While the dependence of calculated and measured bunch length and peak line density are in general very close, it seems that 10% of the impedance is still missing in the present model.

## 4 CURES FOR THE MICROWAVE INSTABILITY

Results from numerical simulations using the impedance model for the SPS discussed above show that after the injection of the LHC

beam into the SPS, bunches with nominal intensity will suffer particle loss along the 7.2 s flat bottom. Raising the voltage adiabatically after injection should improve the situation. However, as there are three consecutive injections from the PS per SPS supercycle, the voltage must be decreased adiabatically back to the matched value before the arrival of the next batch. Better solutions would be the following:

- Increasing the momentum spread of the injected bunches. This requires more RF voltage in the PS and improvement of the transfer line to the SPS. It also raises the capture voltage in the SPS, easing beam loading problems. For the same value of emittance this has the added benefit of reducing the bunch length and reducing the probability of creating the so-called satellite bunches.
- Shielding the accidental cavities created by vacuum ports and septum magnets from the beam. A mechanical solution is under study,[18] but access in the ring to the vacuum ports requires displacing about 400 dipole magnets.
- Increased damping of the cavities created by the vacuum ports should raise the threshold of the instability as it brings the impedance from the narrow band into the broad band regime. From numerical simulations a $Q \leq 10$ would be sufficient to stabilise the nominal beam.
- Decreasing the transition energy in the SPS which raises the threshold in proportion to $\eta$. Attention to this solution was again attracted during the Workshop.[19] This solution requires changing the present operational optics of the SPS and is now under study. Using $\gamma_t = 19.5$ instead of the present 23.4 in numerical simulations eliminates particle losses almost up to the ultimate intensity. An added advantage is the higher capture voltage, 3.4 MV instead of 1.2 MV.
- Increasing the injection energy, which also increases $\eta$, as proposed in this Workshop in the project PSXXI.[20]

## 5 CONCLUSIONS

Measurements of the SPS impedance have been made over a broad frequency range, 100 MHz to 4 GHz, using single bunches injected

into the machine at 26 GeV/$c$. These measurements allowed the dominant impedances with high $R_{sh}/Q$ values, responsible for the single bunch longitudinal instability in the SPS to be seen with the beam. These have shown that a realistic model of the SPS should take account of the narrow band (in relation to the bunch spectrum) nature of the resonant structures in the ring. It has been possible with such a model, which still has to be refined, to explain reasonably well different measurements of the microwave instability threshold. The results of measurements suggest ways of reducing, where possible, the impedance of the dominant elements in the machine – of great importance for preparing the SPS as injector for LHC.

### *Acknowledgements*

We thank T. Bohl and U. Wehrle for their help in taking data, R. Cappi and D. Manglunki for preparing the special beams in the PS and SL Operation Group for setting up the cycles in the SPS.

### *References*

[1] D. Boussard, G. Dome, T. Linnecar and A. Millich, *IEEE Trans. on Nucl. Science*, **NS-24**(3), 1977, p. 1399.
[2] L.R. Evans and J. Gareyte, CERN SPS/85-15 (DI-MST), 1985.
[3] T. Linnecar and E. Shaposhnikova, CERN SL Note/94-87(RF), 1994.
[4] R. Garoby, CERN PS/RF/Note 93-17, 1993.
[5] E. Keil and W. Schnell, CERN/ISR/TH/RF/69-48, 1969; D. Boussard, CERN/LAB/II/RF/75-2, 1975.
[6] D. Boussard and J. Gareyte, Improvement Report No. 181, 24 June 1980.
[7] T. Linnecar and E. Shaposhnikova, CERN SL MD Note 164, 1995, and CERN SL-Note 95-82 (RF), 1995.
[8] T. Bohl, T. Linnecar and E. Shaposhnikova, *Phys. Rev. Lett.*, v. 78, April 21, 1997, p. 3109.
[9] T. Linnecar and E. Shaposhnikova, CERN/SL/93-43 (RFS), 1993.
[10] J. MacLahlan, Fermilab TM-1716, March 1991.
[11] L. Vos, CERN SPS/86-21 (MS), 1986.
[12] T. Linnecar, CERN-SPS/ARF/78-17, 1978.
[13] T. Linnecar and E. Shaposhnikova, CERN SL-Note 96-49 (RF), 1996.
[14] W. Hofle, CERN SL/Note 96-40 (RF), 1996.
[15] J.M. Wang and C. Pellegrini, *Proc. XI Int. Conf. on H.E.Ac. 1980*, p. 554.
[16] K.Y. Ng, *Proc. 1986 Summer Study on Phys. of SSC*, 1986, p. 590.
[17] K.Y. Ng, *Proc. PAC95*, 1995, p. 2977.
[18] J. Ramillon, private communication.
[19] R. Garoby, proceedings of this workshop.
[20] B. Autin, proceedings of this workshop.